

MIT Open Access Articles

*STELLAR POPULATIONS AND RADIAL
MIGRATIONS IN VIRGO DISK GALAXIES*

The MIT Faculty has made this article openly available. *Please share* how this access benefits you. Your story matters.

Citation: Roediger, Joel C., Stephane Courteau, Patricia Sanchez-Blazquez, and Michael McDonald. "STELLAR POPULATIONS AND RADIAL MIGRATIONS IN VIRGO DISK GALAXIES." The Astrophysical Journal 758, no. 1 (September 24, 2012): 41. © 2012 American Astronomical Society.

As Published: <http://dx.doi.org/10.1088/0004-637x/758/1/41>

Publisher: Institute of Physics/American Astronomical Society

Persistent URL: <http://hdl.handle.net/1721.1/95423>

Version: Final published version: final published article, as it appeared in a journal, conference proceedings, or other formally published context

Terms of Use: Article is made available in accordance with the publisher's policy and may be subject to US copyright law. Please refer to the publisher's site for terms of use.



STELLAR POPULATIONS AND RADIAL MIGRATIONS IN VIRGO DISK GALAXIES

JOEL C. ROEDIGER¹, STÉPHANE COURTEAU¹, PATRICIA SÁNCHEZ-BLÁZQUEZ², AND MICHAEL McDONALD³

¹ Department of Physics, Engineering Physics & Astronomy, Queen's University, Kingston, Ontario, Canada;

jroediger@astro.queensu.ca, courteau@astro.queensu.ca

² Departamento de Física Teórica, Universidad Autónoma de Madrid, E-28049 Madrid, Spain; p.sanchezblazquez@uam.es

³ Kavli Institute for Astrophysics and Space Research, Massachusetts Institute of Technology Cambridge, MA, USA; mcdonald@space.mit.edu

Received 2012 January 26; accepted 2012 July 29; published 2012 September 24

ABSTRACT

We present new stellar age profiles, derived from well-resolved optical and near-infrared images of 64 Virgo cluster disk galaxies, whose analysis poses a challenge for current disk galaxy formation models. Our ability to break the age–metallicity degeneracy and the significant size of our sample represent key improvements over complementary studies of field disk galaxies. Our results can be summarized as follows: first, and contrary to observations of disk galaxies in the field, these cluster galaxies are distributed almost equally amongst the three main types of disk galaxy luminosity profiles (I/II/III), indicating that the formation and/or survival of Type II breaks is suppressed within the cluster environment. Second, we find examples of statistically significant inversions (“U-shapes”) in the age profiles of all three disk galaxy types, reminiscent of predictions from high-resolution simulations of classically truncated Type II disks in the field. These features characterize the age profiles for only about a third ($\leq 36\%$) of each disk galaxy type in our sample. An even smaller fraction of cluster disks ($\sim 11\%$ of the total sample) exhibit age profiles that decrease outward (i.e., negative age gradients). Instead, flat and/or positive age gradients prevail ($\geq 50\%$) within our Type I, II, and III subsamples. These observations thus suggest that while stellar migrations and inside-out growth can play a significant role in the evolution of *all* disk galaxy types, other factors contributing to the evolution of galaxies can overwhelm the predicted signatures of these processes. We interpret our observations through a scenario whereby Virgo cluster disk galaxies formed initially like their brethren in the field but which, upon falling into the cluster, were transformed into their present state through external processes linked to the environment (e.g., ram-pressure stripping and harassment). Current disk galaxy formation models, which have largely focused on *field* galaxies, fail to reproduce these results, thus calling for adequate hydrodynamical simulations of dense galaxy environments if we are to understand cluster disks. The current paper highlights numerous constraints for such simulations. In the Appendix, we confirm the claim by Erwin et al. that Type II breaks are absent in Virgo cluster S0s and discuss the detection of Type III breaks in such galaxies.

Key words: galaxies: clusters: individual (Virgo) – galaxies: evolution – galaxies: spiral – galaxies: stellar content – galaxies: structure

Online-only material: color figures

1. INTRODUCTION

The classic paradigm of disk galaxy formation posits that these systems arise through the dissipative collapse of rotating gas clouds (Fall & Efstathiou 1980). If the timescales for star formation and viscosity coincide, then the resultant luminosity distributions within these galaxies should fall off exponentially in the radial direction (Lin & Pringle 1987; Slyz et al. 2002) and stellar ages should either be approximately constant or decrease with galactocentric radius (Ferguson & Clarke 2001; Mollá & Díaz 2005; Naab & Ostriker 2006). Alternatively, an exponential luminosity distribution could arise from a combination of supernovae feedback, variation in the angular momentum distribution of halo gas, and inefficient star formation at low gas densities (Dutton 2009). Either way, galaxies showing such surface brightness profiles are commonly referred to as “Type I” disks (Freeman 1970; Bland-Hawthorn et al. 2005). Statistical studies of luminosity profiles in field galaxies (e.g., Pohlen & Trujillo 2006, hereafter PT06; Erwin et al. 2008, hereafter Er08) have revealed that Type I disks in the field are rare (Type I fraction, $f_I \sim 20\%$; Gutiérrez et al. 2011, hereafter Gu11). Disk galaxy luminosity profiles are instead mostly characterized by two exponentials (“Type II”; van der Kruit 1979; de Grijs et al. 2001; Pohlen et al. 2002), the outer exponential being shallower than the inner one; the Type II fraction, f_{II} , is roughly 50% (Gu11).

The transition between those two (nearly) exponential parts of a galaxy luminosity profile is referred to as the “break” radius. The opposing case, where the outer disk profile is shallower beyond the break, is referred to as a “Type III” disk (Erwin et al. 2005) and occurs with a frequency comparable to field Type IIs ($f_{III} \sim 30\%$; Gu11). It is worthwhile to note that the fractions of the three disk galaxy types within other environments (i.e., groups and clusters) remain poorly known (but see Maltby et al. 2012 and Erwin et al. 2012).

The nature of Type IIIs is not yet well understood but some have speculated that their breaks represent either the transition from the disk to an outer spheroid (Erwin et al. 2005) or the aftermath of minor mergers onto gas-rich disks which promoted stars from the progenitors to the remnants’ outskirts (Younger et al. 2007). Conversely, the range of morphology in spiral disks with Type II breaks in PT06 suggests that a variety of mechanisms can generate such breaks in disk galaxies, yet only that pertaining to truncated star-forming disks, for so-called classical truncations (hereafter “Type II-CT” disks), has been studied in earnest thus far. The ensuing discussion provides a broad overview of our current knowledge about the formation of such galaxies.

The luminosity profile breaks in Type II-CTs have historically been attributed to either angular momentum thresholds during the formation of disk galaxies (van der Kruit 1987; van den

Bosch 2001), angular momentum redistribution via subsequent secular evolution of assembled disks (Debattista et al. 2006; Bournaud et al. 2007; Foyle et al. 2008), or a density-dependent star formation law (Kennicutt 1989; Elmegreen & Parravano 1994; Schaye 2004). Although the redistribution scenario can account for the large scatter in the age–metallicity plane for stars within the solar neighborhood (Edvardsson et al. 1993; Haywood 2008) (i.e., chemical evolution models without redistribution fail to reproduce the observed scatter; Wielen et al. 1996; Sellwood & Binney 2002), the fact that ultraviolet emission is frequently detected beyond the optical extent of many disk galaxies (including Type IIs; Gil de Paz et al. 2005; Thilker et al. 2007) strongly suggests that in situ star formation contributes on some level to building the stellar mass in their outer regions. Thus, it is quite likely that some hybrid of the above scenarios (e.g., angular momentum redistribution plus density-dependent star formation) is likely responsible for the existence of Type II-CT disks.

Various models have been proposed to explain the redistribution of angular momentum that may assist in the formation of Type II-CT disks. One such model attributes this redistribution to an increase in the random velocities of disk stars caused by gravitational interactions with molecular clouds (Spitzer & Schwarzschild 1953; Wielen 1977; Wielen et al. 1996), but it fails to reproduce the aforementioned scatter in the Galactic age–metallicity relation (Nordström et al. 2004). Alternatively, individual disk stars can have their angular momentum redistributed by changing the guiding centers of their orbits. So-called radial migrations of stars can be produced by a number of mechanisms, the first being postulated by Sellwood & Binney (2002) in the context of resonant scatterings of disk stars off of transient spiral density waves. Given a superposition of several spiral patterns, Sellwood & Binney showed that significant displacements ($\lesssim 4$ kpc) of guiding centers could be achieved. Minchev & Famaey (2010) further argued that an overlap of bar and spiral-arm resonances could drastically enhance the efficiency of migration within a Milky Way-like disk, mixing it within ~ 3 Gyr (see also Debattista et al. 2006). Lastly, Quillen et al. (2009) showed that radial migrations of stars to the outskirts of galaxy disks could arise via tidal perturbations during the pericenter passages of dwarf satellites (e.g., Sgr dSph; see also Bird et al. 2012). Although its efficiency remains to be quantified, this mechanism fits quite naturally within the current cosmological paradigm. Overall, and given the many mechanisms through which radial migrations can be incited, can observations of external galaxies distinguish between them?

The Sellwood & Binney (2002) resonant scattering mechanism was revisited by Roškar et al. (2008, hereafter R08) through their high-resolution simulation of an idealized galaxy disk which included both gas and star formation. Their disk rapidly developed a Type II-CT break that persisted over several dynamical times, the origin of which was linked to the combination of angular momentum conservation within the collapsing gas cloud, a surface density threshold in their star formation recipe, and radial migrations populating the region beyond the break with inner disk stars. Given the inside-out growth of the inner disk and that the diffusion length for stars scales with the square root of their age, R08 found that the stellar age profile of their simulated disk was described by both a negative and positive gradient interior and exterior to its break, respectively. In the wake of that study, Martínez-Serrano et al. (2009, hereafter MS09) and Sánchez-Blázquez et al. (2009, hereafter SB09) investigated the formation of Type II-CT breaks in the

context of *cosmological* simulations. While these authors also found “U-shaped” age profiles for their model disks associated with rapid decreases in the gas densities beyond their break radii, SB09 showed that the decrease in their simulation arose from the onset of a warp in the gas disk at the break rather than an angular momentum threshold (i.e., it is physically well motivated). It is also worth stressing that the above simulations focused on relatively isolated systems; comparable simulations for cluster galaxies are currently lacking.

While the above simulations of Type II-CT disk formation uniformly suggest that these galaxies are described by U-shaped stellar age profiles, such radial age inversions have only been explicitly detected in three Type II galaxies so far (NGC 2684, NGC 6155, and NGC 7437) by Yoachim et al. (2010, 2012), while the age profiles for the remaining Type IIs in their sample which could be measured beyond their respective breaks (IC 1132, NGC 4904, and NGC 6691) do not exhibit a significant increase with radius in those regions. Furthermore, amongst their positive detections, these authors found that the inversion occurs well within the break in all cases. Other detections of inverted age profiles have also been achieved through studies of the resolved stellar populations of three nearby Type II galaxies (M33, NGC 4244, and NGC 7793; de Jong et al. 2007; Williams et al. 2009; Barker et al. 2011; Radburn-Smith et al. 2012), albeit by somewhat indirect means, such as surface brightness profiles for different age groups of stars or distributions of stellar age/star formation rate for several *Hubble Space Telescope* (HST) fields. Bakos et al. (2008) and Azzollini et al. (2008) have both claimed age inversion detections in larger samples of nearby and distant Type II galaxies, respectively, given that their color profiles invert at their break radii. These findings, however, were benchmarked on optical colors, the translation of which into ages is fraught with uncertainty due to the well-known age–metallicity degeneracy. Signal-to-noise constraints also required stacked color profiles rather than those of individual galaxies (as we do here). Lastly, in their stellar population analysis of S0 galaxies, Prochaska Chamberlain et al. (2011) found that nearly a quarter of their sample exhibited very old ages in their outskirts, consistent with the above predictions and detections of U-shaped age profiles.

Despite their intrinsic uncertainties, stellar population data are, in principle, ideal to test the predictions of existing disk galaxy formation models. Such a test represents a key step toward a definitive picture of many observable properties of disk galaxies, including Type II-CT breaks, and whether they arise from a density-dependent star formation law, angular momentum thresholds or redistribution, or some combination thereof. The intent of this work is to present such a test in the context of all three types of disk galaxies by taking advantage of our recent analysis of both the luminosity and stellar population profiles of Virgo cluster galaxies (McDonald et al. 2011; Roediger et al. 2011a). Although hydrodynamic models of disk galaxies which include radially resolved stellar age information only exist for field environments,⁴ comparing their predictions against our data can still be insightful toward fashioning an understanding of the role of environment on the evolution of these galaxies (i.e., nature versus nurture) and constraining future models of cluster evolution. Specifically, we aim to increase the number of explicit detections of U-shaped age profiles in all disk galaxy types, thereby bolstering the

⁴ Hydrodynamic models of cluster galaxies have thus far mostly addressed the study of ram-pressure stripping (Abadi et al. 1999; Vollmer et al. 2001; Roediger & Hensler 2005; McCarthy et al. 2008).

empirical evidence that radial migrations are a generic aspect of galaxy evolution, while simultaneously drawing attention to cases of nondetections and the very plausible notion that other evolutionary processes (perhaps tied to environmental effects, such as ram-pressure stripping) may either prevent or obliterate age inversions in galaxies. The latter goal is made all the more imperative given the intriguing results achieved by Yoachim et al. (2010, 2012) described above. To our knowledge, the present work is a first attempt toward explicitly studying stellar populations as a function of disk galaxy type in the context of current generation galaxy formation models and within the cluster environment.

We highlight in Section 2 various aspects of our database of Virgo galaxies’ luminosity and stellar population profiles which pertain to this study and present, in Section 3, our data analysis in the context of Type I, II, and III disk galaxy formation models. Conclusions are presented in Section 4. We examine in the Appendix the recent claim by Erwin et al. (2012, hereafter Er12) that cluster S0 galaxies do not exhibit Type II breaks.

2. DATA

Our investigation into the origins of the three principal disk galaxy types in dense environments stems from our recent analysis of the radially resolved colors and stellar populations of a complete, magnitude-limited sample of 283 Virgo cluster galaxies spanning all manner of morphological types and surface densities (Roediger et al. 2011a, 2011b). This analysis was facilitated by the availability of optical (*gri*) and near-infrared (*H*) luminosity profiles for the aforementioned sample from McDonald et al. (2011). In Roediger et al. (2011a), we appealed to stellar population models corresponding to an exponential star formation history of variable timescale and a broad range of metallicities to homogeneously convert those optical–infrared luminosity profiles into estimates of the underlying mean stellar age and metallicity profiles for all 283 galaxies. These luminosity, age, and metallicity profiles enabled the present work. The reader may consult McDonald et al. (2011)⁵ for the presentation of our luminosity profiles and Roediger et al. (2011a) for further details about our adopted stellar population models and the derivation of our age and metallicity profiles.

Our Type I, II, and III subsamples are drawn from the 85 disk galaxies in the Virgo cluster survey of McDonald et al. (2011). Their morphological types were taken from the NASA Extragalactic Database⁶ (NED; i.e., Sa–Sm, Im morphologies). For reasons described in the Appendix, the 55 S0 galaxies in the McDonald et al. sample were left out of this analysis. Of the initial sample of 85 disk galaxies, we discarded 14 on account of severe dust extinction (which would skew their stellar population diagnostics), another 4 due to clear signs of strong overlap/interaction with neighboring systems or contamination by a bright foreground star/H II region (yielding artificial Type III luminosity profiles), and three others which were too faint for their stellar populations to be reliably modeled. These various cuts leave us with a sample of 64 bona fide, largely noninteracting Virgo cluster disk galaxies with low to moderate attenuation and high-quality optical–infrared luminosity profiles, in order to analyze both the broad structures and stellar populations of their disks.

The *griH* luminosity profiles for each of our disk galaxies were inspected visually by the authors and classified according

Table 1

Luminosity Profile Types as a Function of Morphology for Virgo Disk Galaxies

Type	Fraction per Morphological Bin (%)			Total Fraction (%)
	Sa–Sbc	Sc–Sm	Im	
(1)	(2)	(3)	(4)	(5)
I	0.03	0.14	0.14	0.31
II	0.09	0.14	0.11	0.34
III	0.19	0.12	0.03	0.34

to their Type I/II/III features and following the detailed schemes of PT06 and Er08 (however, see footnote 10 in Section 3.2.). Specifically, a galaxy was assigned a Type I, II, or III class if its luminosity profile could be adequately described by a single exponential drop-off from the intermediate to outer regions of the galaxy (Type I) or exhibits a sharp break from an inner exponential section to either a steeper (Type II), or yet a shallower (Type III) one at some common radius amongst all bands. If the aforementioned break is not seen at all bands, *including* the near-infrared, or if it occurs in a section of the luminosity profile that is dominated by sky errors (where the profile point-to-point fluctuations are comparable to sky flux errors), then no physical or statistical basis exists for claiming that the associated galaxy be classified as anything other than a Type I. On that basis, many of our galaxies are better classified as Type Is rather than IIIs since profile breaks in the latter typically occur at low surface brightnesses ($27\text{--}28\text{ mag arcsec}^{-2}$ at *i* band) where sky errors are dominant. Fortunately, these issues do not affect our reported Type II disks.

Altogether, we find that our sample of Virgo cluster disk galaxies consists of ~ 20 Type Is, 22 Type IIs, and ~ 22 Type IIIs.⁷ Figure 1 shows the *i*-band images for our Type II subsample, where the ellipses denote the locations of the breaks (red) and probable extents of the bars (green; if present, as gauged by eye) in these systems, while in Table 1 we present the fractions of our Type I, II, and III subsamples contributed by each of the principal disk morphological types (Sa–Sb, Sbc–Sm, and Im), normalized to our total disk sample (i.e., the sum of all of the fractions is unity). The morphological breakdown in Table 1 shows that our Type I and III subsamples are largely comprised of late-type disks and irregulars, and early- and late-type disks, respectively, while our Type II subsample contains a range of morphologies. Conversely, Table 1 also shows that our early-type disks are mostly described by Type III profiles, while our late-type disks and irregulars are comprised of nearly-equal fractions of Type I–III and Type I–II profiles, respectively. These results conflict with Gu11, Er08, and PT06, who found that 28%/27%/10%, 21%/48%/60%, and 51%/24%/30% of S0–Sb/SB0–SBb/Sb–Sdm galaxy types possess Type I, II, and III profiles, respectively, and that the fraction of Type Is and IIs per morphological bin decreases and increases from early to late galaxies, respectively, while that for Type IIIs varies between 20% (Sa, Sd, Sm) and 50% (S0, Sb). *The resolution of this conflict most likely lies in the fact that PT06, Er08, and Gutiérrez et al. targeted field galaxies, whereas our sample is drawn from a cluster environment.* Indeed, Er12 recently reported a complete dearth of Type II profiles amongst Virgo S0s, while Moore et al. (1999) showed that multiple flybys between cluster galaxies (so-called harassment) can transform Type I disks into Type IIIs. These pieces of evidence, paired with our Type I/II/III statistics, provide initial support for the main

⁵ <http://www.astro.queensu.ca/~virgo>

⁶ <http://ned.ipac.caltech.edu>

⁷ The Type I and III numbers are somewhat uncertain since deeper imaging for these galaxies (Ferrarese et al. 2012) could call for a type revision.

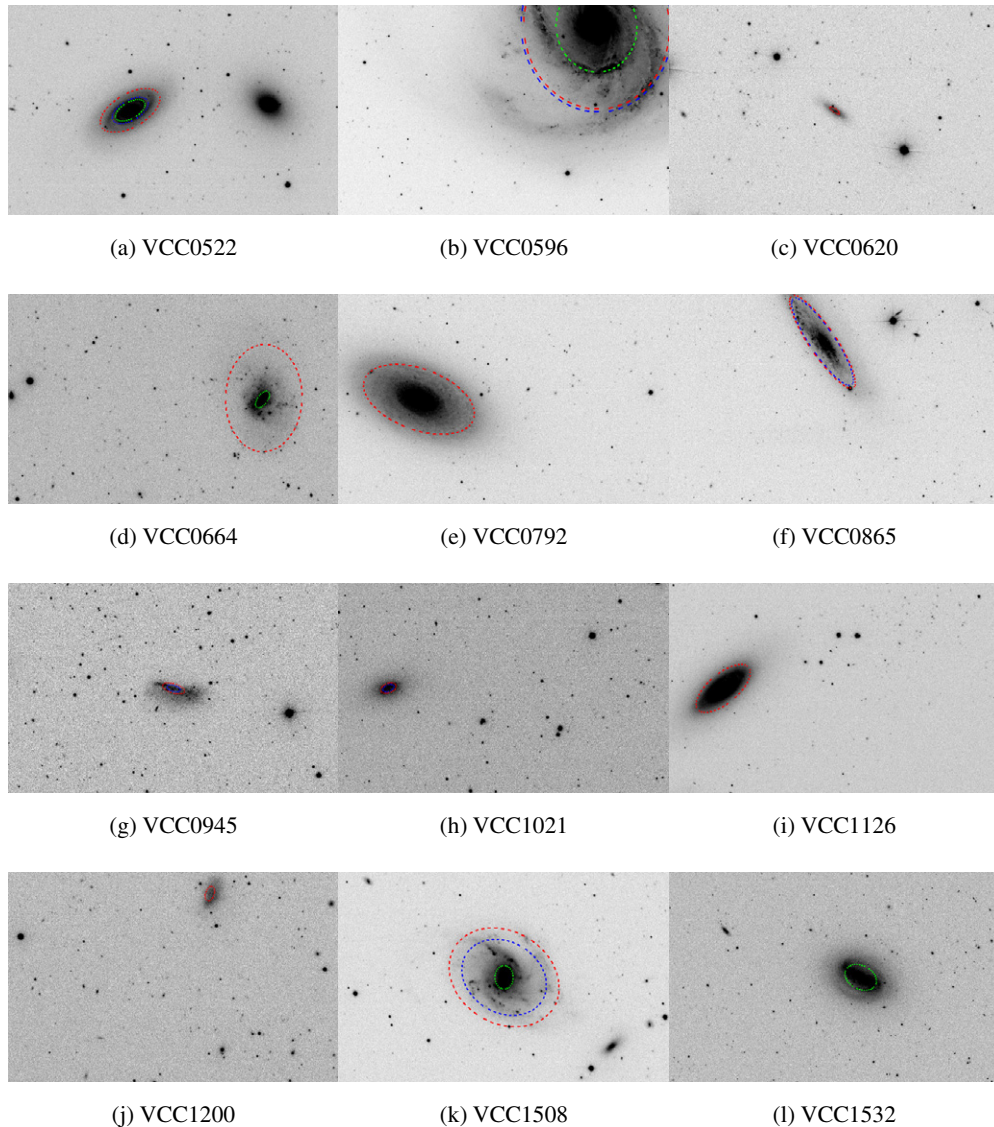


Figure 1. *i*-band images for our subsample of Virgo Type II galaxies. The overlaid ellipses correspond to either the locations of the luminosity profile breaks (red) or mean stellar age profile minimum (if present; blue), or the extents of the bars (if present; green) within these systems. The images are shown on a common pixel scale and have the same dimensions.

theme of the present paper: that the evolution of disk galaxies is substantially (and verifiably) different in field versus cluster environments (see Section 5 in Er12). This conclusion should stand even if deeper optical imaging for larger samples of Virgo disk galaxies (Ferrarese et al. 2012) should reveal an increase in the number of Type III systems within this cluster (at the expense of the Type I fraction), as it is truly the relative absence of Type II disks in Virgo that stands out.

We present in Figures 2–4 the *griH* surface brightness profiles of our Type I, II, and III systems (*g* = blue, *r* = green, *i* = orange, and *H* = black). The Virgo Cluster Catalog (VCC) galaxy numbers from Binggeli et al. (1985), detailed morphological classifications from NED, and, for our Type IIs alone, specific Type class (e.g., II-o.CT) have been included in all panels, as well as the break locations for our Type II and III subsamples (red vertical lines). We also show in each panel the 1σ sky error envelope of the *i*-band data set (black continuous line) to illustrate the importance of such envelopes in evaluating the behavior of disk galaxies’ luminosity profiles in their outskirts: again, if the extrapolation of the inner (mostly

exponential) profile to the galaxy’s outskirts falls within its sky error envelope, then no statistical basis exists for claiming that that disk is anything but a Type I. Other cautionary cases also exist. For instance, the apparent Type II breaks found at $30''$ in the profiles for VCC 1326 and 1811 (both Type Is) are due to the isophotal contours intercepting the edge of a bar and spiral arm at these locations, respectively, while the apparent Type III break at $25''$ in the profiles for VCC 1508 (a Type II) most likely marks the transition from its bulge to its disk. This and many other galaxies in our Type II subsample do appear to host Type III breaks further out in their disks; however, we nevertheless retain them in that subsample (and simply identify them as Type II+IIIs) as we suspect that they fell into the cluster as Type IIs but developed their Type III breaks via harassment (Moore et al. 1999). The existence of these exceptional cases reinforces the notion that classification of disk galaxy luminosity profiles remains a somewhat subjective process and, as such, must be performed and interpreted with care.

As to the role that sky error envelopes play in determining a disk galaxy’s type, we examine in our Appendix the recent claim

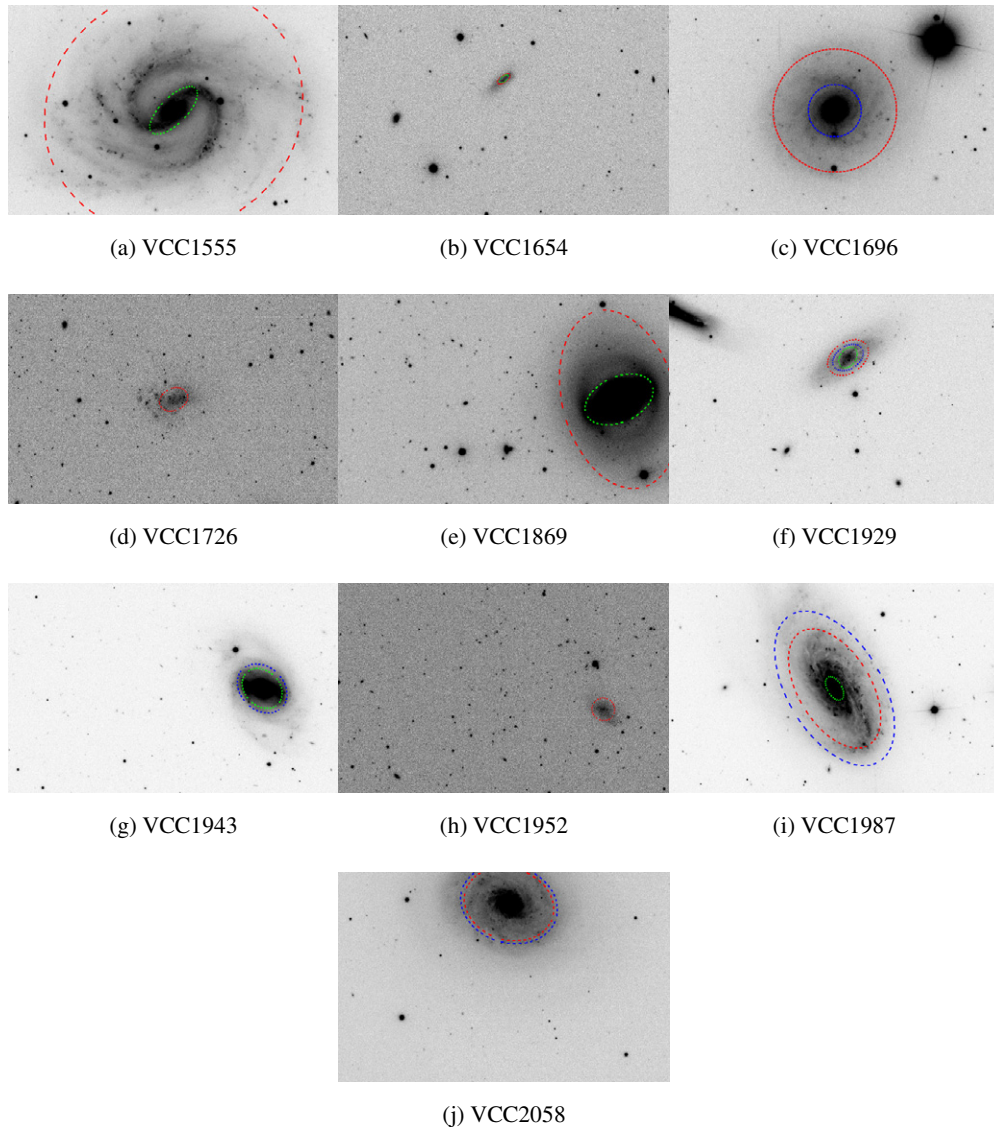


Figure 1. (Continued)

by Er12 that roughly half of all bright Virgo S0s possess Type III disks. It will be found that, at least for those galaxies where our respective samples overlap, many of Er12’s Type III detections depend critically on the assumed sky level and could be labeled as pure Sérsic systems with $n > 1$. Still, their reported lack of Type II systems and existence of at least some disk upturns (Type IIIs) in cluster S0 galaxies appear to be genuine.

3. RESULTS AND DISCUSSION

3.1. Type Is

The mean stellar age profiles of our 20 Type I galaxies are shown in Figure 5, where galactocentric radii have been expressed in terms of both physical (kpc; bottom axis) and effective (r_e ; top axis) units, assuming a distance of 17 Mpc to the Virgo cluster (Mei et al. 2007). We find that the majority of these galaxies are characterized by age gradients (change in age per unit radius) which are either positive or flat (40% and 35% of our Type I subsample, respectively). This contrasts with most Type I formation models which predict that these galaxies form from inside-out (Ferguson & Clarke 2001; Mollá & Díaz 2005; Naab & Ostriker 2006; Dutton 2009), implying that they

should harbor *negative* age gradients, whereas such gradients are only found in two of our Type Is (10%). Some nuances in these models actually allow for flat (Ferguson & Clarke 2001) or positive (Robertson et al. 2004) age gradients within purely exponential disks depending on whether star formation begins during or after the assembly of the gas disk, or if gas-rich minor mergers/accretion events occur at late epochs, respectively. Unfortunately, high-resolution hydrodynamic models to tackle the case of disk galaxy formation and/or evolution within the cluster environment are still lacking. Based on the above observations, one then wonders if existing models (largely geared toward isolated galaxies and most often predicting negative age gradients) can reproduce the high frequency of positive and flat age gradients when cast in the context of denser galaxy environments.

Short of appropriate models to compare our observations, we may speculate that the preponderance of flat and positive age gradients in Virgo Type Is is an artifact of the galaxy environment; cluster galaxies experience a variety of physical processes that field galaxies do not. For instance, by removing the gas from and thereby quenching star formation in the outskirts of a galaxy disk, it is conceivable that ram-pressure stripping via the

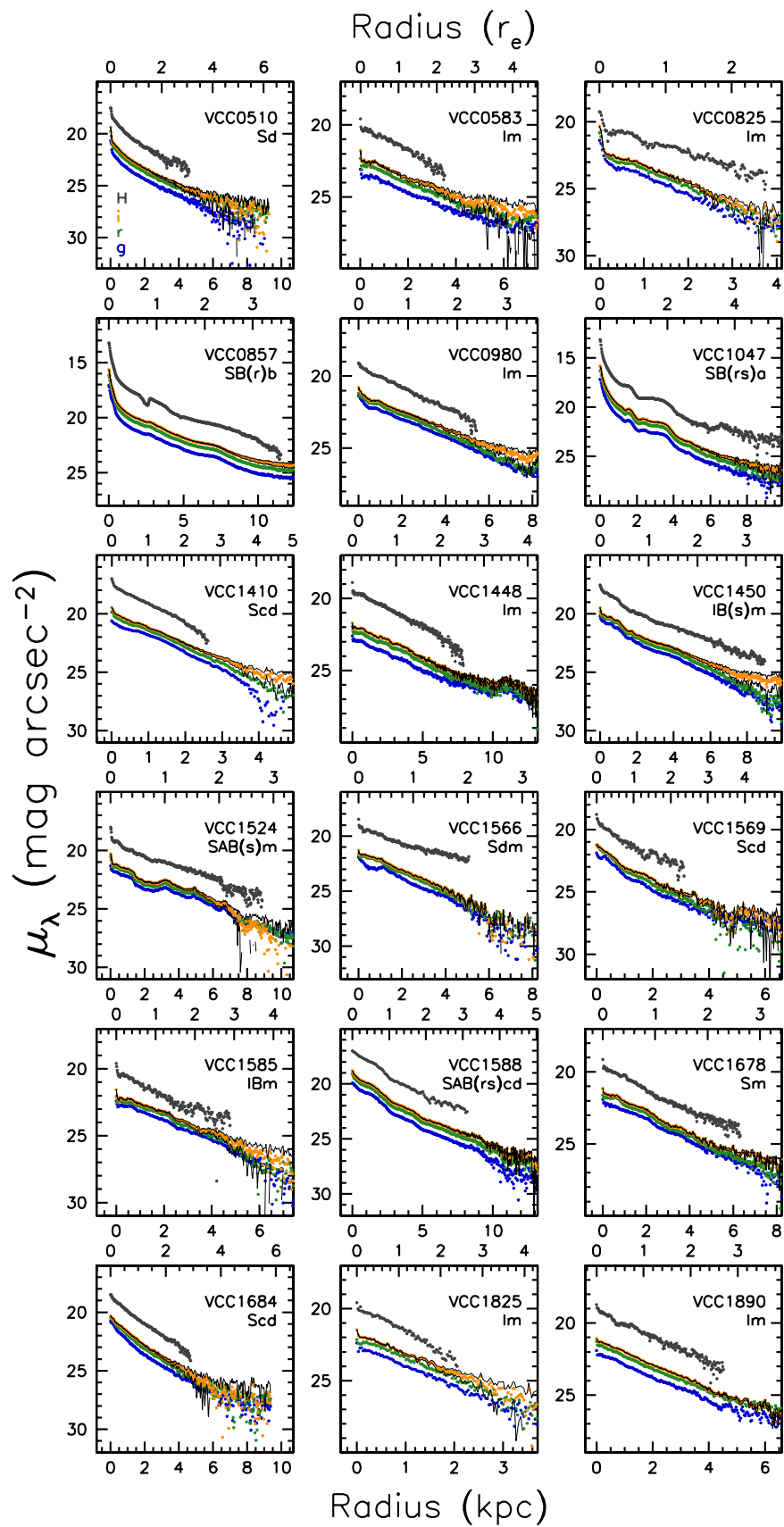


Figure 2. Surface brightness profiles in the *griH* bands for our subsample of Virgo Type I galaxies (*g* = blue; *r* = green; *i* = orange; *H* = black). The VCC (Binggeli et al. 1985) identification number and detailed morphology is provided for each galaxy, while radii are quoted in terms of *H*-band effective radii (McDonald et al. 2009) and kiloparsecs on the top and bottom of each panel, respectively. The 1σ sky error envelope for each galaxy’s *i*-band profile is shown as the black continuous line in each panel.

(A color version of this figure is available in the online journal.)

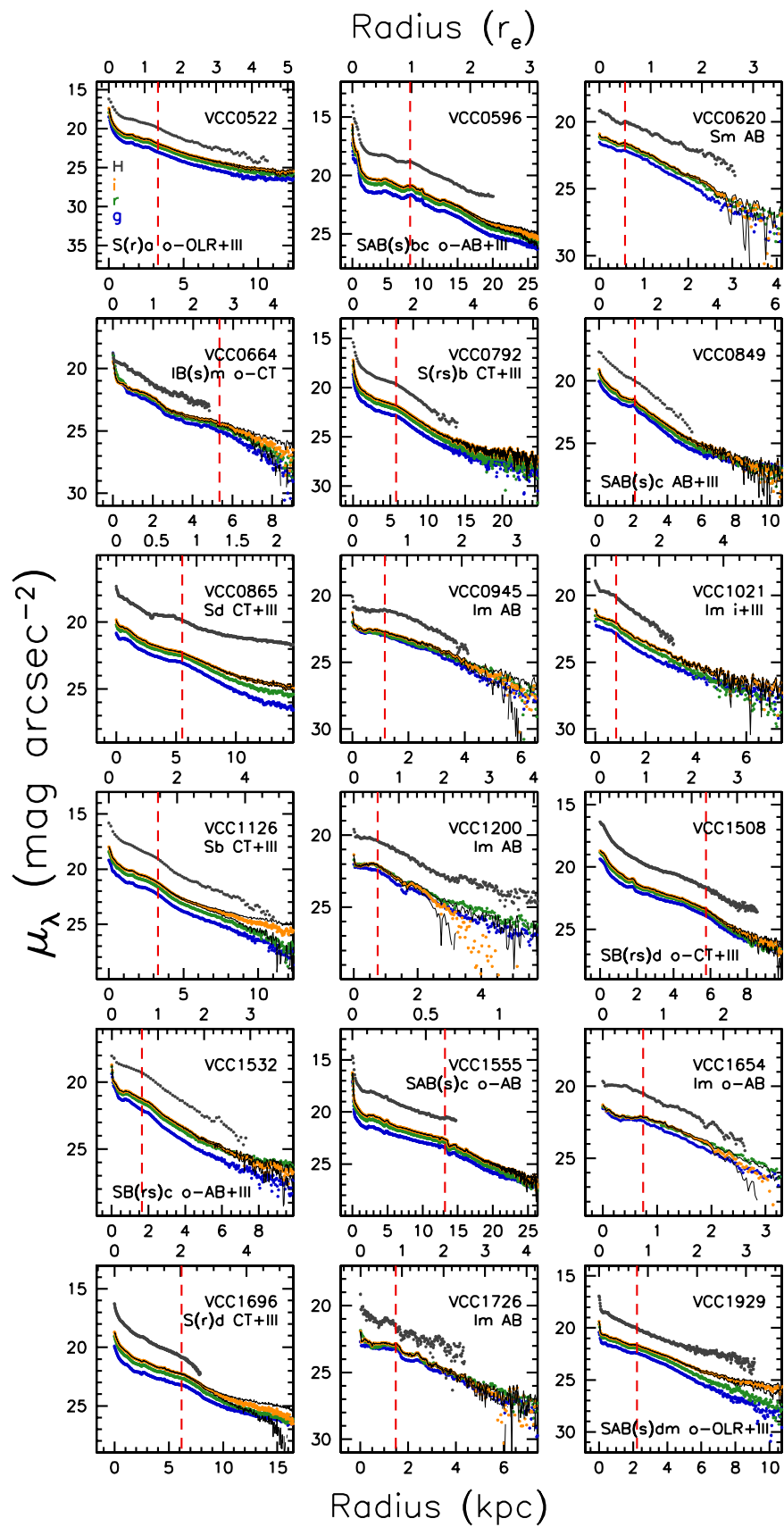


Figure 3. As in Figure 2 but for Virgo Type II galaxies. The specific class of Type II break has also been provided, while the location of the break for each galaxy is marked by the red vertical line.

(A color version of this figure is available in the online journal.)

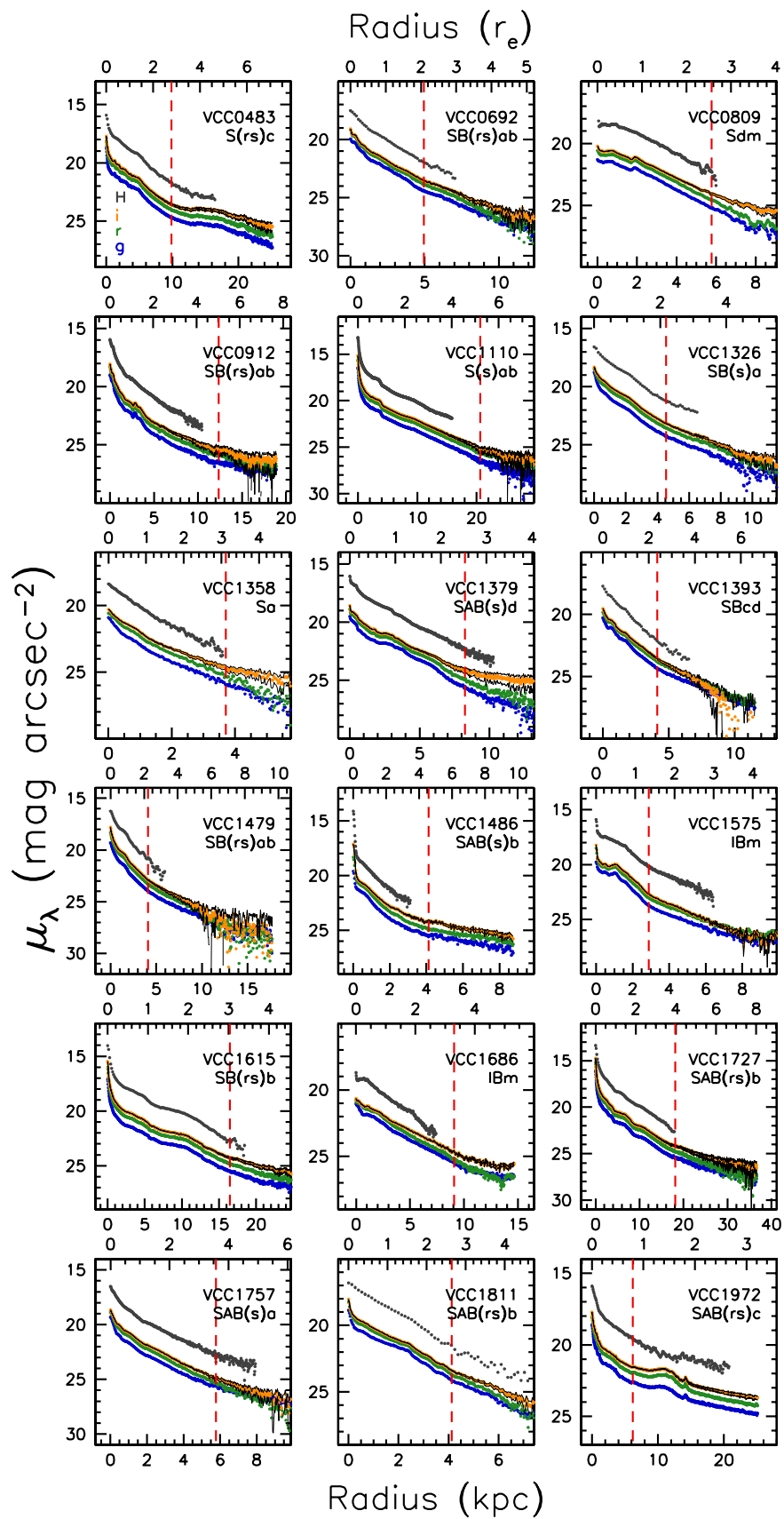


Figure 4. As in Figure 2 but for Virgo Type III galaxies. The location of the break for each galaxy is marked by the red vertical line. (A color version of this figure is available in the online journal.)

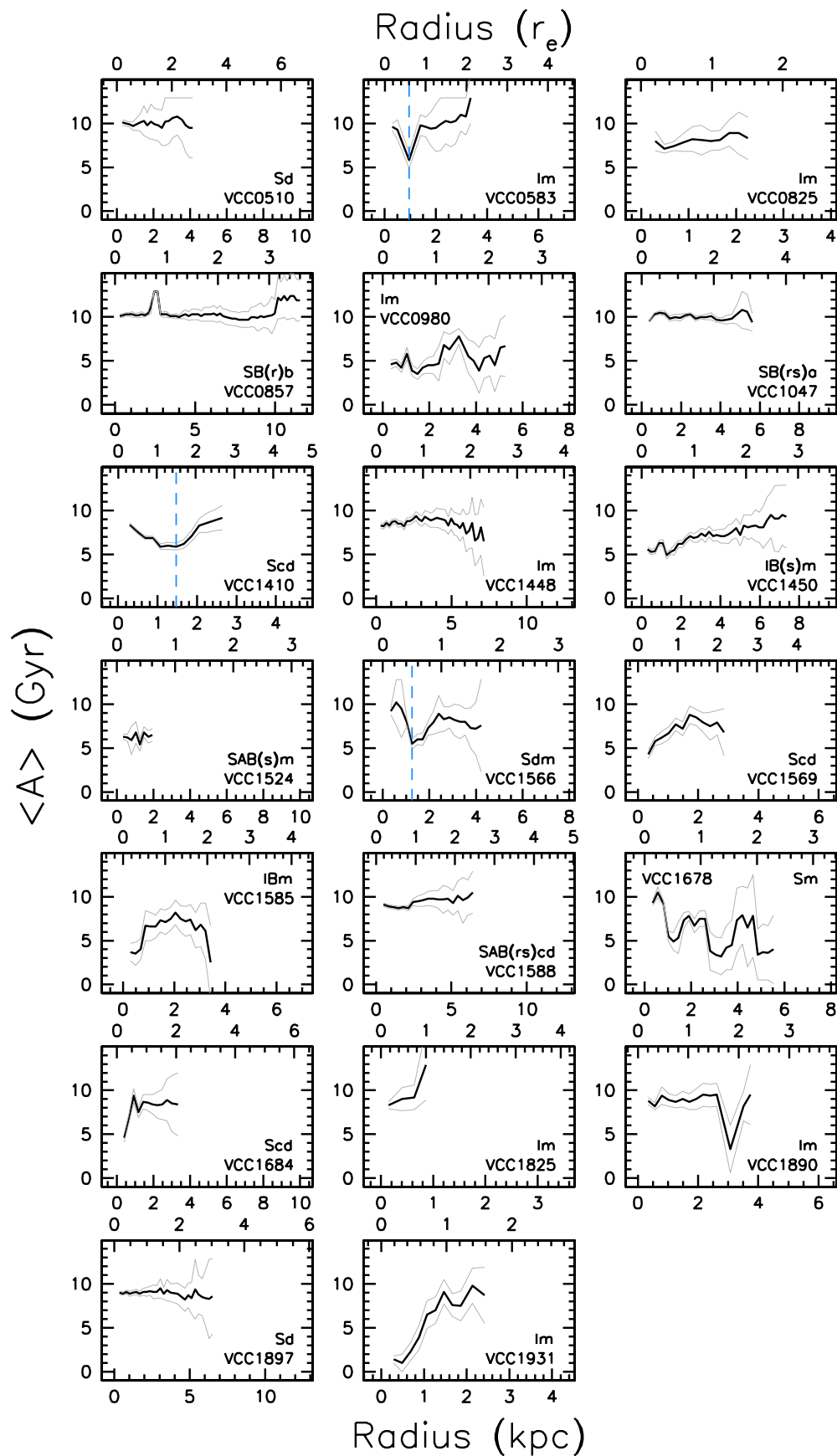


Figure 5. Mean stellar age profiles (black lines) and their 1σ error envelopes (gray lines) for our subsample of Virgo Type I galaxies. The VCC identification number and detailed morphology of each galaxy is provided in each panel, while the location of the age minimum (where applicable) is marked by the blue, dashed vertical line. The ranges along the horizontal axes match those used in the corresponding panels of Figure 2.

(A color version of this figure is available in the online journal.)

Table 2
Age Gradient Distributions for Virgo Disk Galaxies

Type	Age Gradient Fraction (%)			
	Flat	Positive	Negative	U-shaped
(1)	(2)	(3)	(4)	(5)
I	0.40	0.35	0.10	0.15
II	0.14	0.36	0.14	0.36
III	0.23	0.32	0.09	0.36

intercluster medium could evolve a negative age gradient into either a flat or positive one. The two possible outcomes would depend on the galaxy’s ability to retain a central gas reservoir, thus maintaining star formation there. Our knowledge of these galaxies’ neutral gas deficiencies, Def_{HI} ,⁸ remains incomplete, however, while the Type Is with flat or positive age gradients whose Def_{HI} values are known (Gavazzi et al. 2005) are spread over a range >1 dex in this parameter. This seems inconsistent with our above hypothesis. Since Def_{HI} measures the atomic gas content of cluster disks relative to their field (isolated) counterparts, galaxies having more positive Def_{HI} values would have presumably lost proportionally more of their cold gas to ram pressure than systems with more negative Def_{HI} values and, therefore, should host more evolved stellar populations throughout their volumes. Galaxy–galaxy or galaxy–cluster harassment (Moore et al. 1996, 1999), on the other hand, may offer an attractive alternative, at least for flat age gradients, if the tidal forces can promote effective mixing of stellar disks. We revisit this issue in Section 3.4.

Even more tantalizing than the (unexpected) high incidence of flat and positive age gradients in Virgo Type Is is the existence of U-shaped age profiles in the remaining three (15%) galaxies from this subsample (VCC 0583, 1410, and 1566 in Figure 5), akin to those found in simulations of field Type II-CT disks (R08; MS09; SB09). The hallmarks of such age profiles—their minima—are identified (where they occur) in Figure 5 by the blue vertical lines. Although the location of each age minimum was determined by eye, its manifestation was only deemed legitimate if the age gradient interior and exterior to it was computed to be negative and positive, respectively. That is, an age profile minimum is deemed meaningful only if a statistically genuine U-shape can be defined for the profile. With this in mind, we measured the age gradients interior and exterior to each of the identified minima in Figure 5 (via bootstrap linear least-squares fitting) and found that they all satisfy the above stipulations and, most importantly, they are statistically different from zero. To avoid the effects of atmospheric blurring in our interior age gradient measurements, we neglected the centermost data point from each of the galaxy age profiles; in Roediger et al. (2011b) we showed that, for each galaxy in our sample, this data point encloses the maximum seeing disk. The fraction of our Type I subsample which exhibit U-shaped age profiles, or not, are shown in Table 2, while the age gradients and locations of age profile minima (r_{Min} , where applicable) for these galaxies are presented in Tables 3 and 4, respectively. No error on the inner age gradient for VCC 0583 is quoted because the number of data points interior to its age minimum was too low to bootstrap the profile fit in that region; the value of that gradient for VCC 0583 in Table 3 was instead obtained via a simple linear least-squares fit.

⁸ Def_{HI} is a popular metric for measuring the degree of ram-pressure stripping suffered by cluster galaxies (Haynes & Giovanelli 1984).

Table 3
Inner and Outer Mean Stellar Age Gradients for Virgo Disk Galaxies Hosting U-shaped Age Profiles

VCC ID	$d \langle A \rangle / dr_i$ (Gyr kpc ⁻¹)	$d \langle A \rangle / dr_o$ (Gyr kpc ⁻¹)
(1)	(2)	(3)
Type I		
0583	−5.70	+1.78 ± 0.51
1410	−2.13 ± 0.40	+3.05 ± 0.38
1566	−6.88 ± 1.80	+0.56 ± 0.30
Type II		
0596	−0.32 ± 0.02	+0.05 ± 0.02
0849	−3.61 ± 0.72	+1.25 ± 0.42
0865	−0.19 ± 0.04	+0.56 ± 0.02
1021	−2.04	+1.29 ± 0.29
1654	−1.09	+4.72 ± 0.95
1929	−0.58 ± 0.18	+0.54 ± 0.07
1943	−0.59 ± 0.16	+0.35 ± 0.11
1987	−0.40 ± 0.03	+0.48 ± 0.02
Type III		
0692	−2.04 ± 0.78	+0.88 ± 0.30
0912	−0.78 ± 0.34	+0.31 ± 0.04
1379	−0.60 ± 0.11	+1.10 ± 0.11
1686	−1.82 ± 0.37	+2.26 ± 1.18
1811	−1.67 ± 0.46	+0.54 ± 0.23
2012	−0.28 ± 0.08	+0.42 ± 0.35

Table 4
Morphologies, Effective Radii, and Age Minimum Radii (When Present) for Virgo Type I Galaxies

VCC ID	Hubble Type	r_e (kpc)	r_{Min} (kpc)	
(1)	(2)	(3)	(4)	(r_e) (5)
0510	Sd	1.495
0583	Im	1.594	1.795	1.126
0825	Im	1.492
0857	SB(r)b	3.209
0980	Im	2.272
1047	SB(rs)a	1.831
1410	Scd	0.985	1.469	1.492
1448	Im	3.120
1450	IB(s)m	2.647
1524	SAB(s)m	3.179
1566	Sdm	2.510	1.257	0.501
1569	Scd	1.320
1585	IBm	1.645
1588	SAB(rs)cd	2.619
1678	Sm	2.412
1684	Scd	1.615
1825	Im	0.860
1890	Im	1.673
1897	Sd	2.157
1931	Im	1.530

Our discovery of statistically significant inversions in the age profiles in three members of our Type I subsample challenges existing formation models for these galaxies; the latter models have never predicted such stellar population trends. Although sites of recent star formation in disk galaxies (e.g., spiral arms) could presumably depress the mean stellar ages in those regions, such effects, on their own, should not create the kind of *global* minima that we have found in these galaxies’ age profiles. Moreover, ours is not the first detection of such peculiar behavior

in the stellar populations of Type I disks. For instance, Vlajić et al. (2009) found that the stellar metallicity profile for the canonical (field) Type I disk galaxy, NGC 300, inverts from a negative gradient to a positive one, analogous to our findings for our three peculiar Type Is, albeit at a much larger galactocentric radius (10 kpc) and in terms of metallicity rather than age. Guided by simulations which suggest that U-shaped radial distributions of stellar population properties in disk galaxies are a telltale sign of stellar migrations, we might speculate that these Virgo Type Is represent a subpopulation of Type IIs whose outer disks were fully populated by a very efficient migration episode. Clearly though, the existence of this peculiar galaxy population ought to motivate further exploration of Type I galaxy formation models.

3.2. Type IIs

The mean stellar age profiles of our 22 Type II galaxies are shown in Figure 6. We find that the behaviors of these galaxies' profiles are most often described by either positive age gradients or statistically significant U-shapes (each amounting to 36% of the subsample⁹; Table 2), where the latter are reminiscent of predictions from current models of Type II-CT disk formation. The locations of the breaks and age minima in our Type II systems are shown (where applicable) by the red and blue ellipses in Figure 1 and the orange and blue vertical lines in Figure 6, respectively. As for our Type I subsample, detections of U-shaped age profiles were only deemed legitimate if the age gradients interior and exterior to each of the minima identified in Figure 6 were measured via bootstrap linear fitting to be negative and positive, respectively, and statistically different from zero. In all identified cases, the fitted gradients agree with these criteria, as seen from Table 3. Although the central data points from these galaxies' inner age profiles were typically neglected during this procedure, we preserved them for VCC 1021 and 1654 in order to measure their inner age gradients; as before, though, no bootstrap errors are reported for them in Table 3. While these two galaxies' inner gradients should be treated as upper limits, their specific values do not affect our conclusions.

We summarize in Table 5 pertinent information for our Type II subsample, including the locations of their breaks (r_{Brk}) and age profile minima (r_{Min} ; where applicable), both of which are listed in terms of physical units (kpc) and relative to these galaxies' H -band effective radii, r_e , from McDonald et al. (2009). The profile breaks are located within the effective radii for half of this subsample, while the remainder of our Type IIs exhibit their breaks mostly within the 1–2 r_e annulus. In terms of physical units, however, the distribution of break radii seems bimodal, with these galaxies clustering about $r_{\text{Brk}} < 2$ kpc or $r_{\text{Brk}} = 5$ –6 kpc. For those Type IIs with U-shaped age profiles, we find that they do not distinguish themselves from the whole subsample in terms of either r_{Brk} or any of the nonparametric quantities measured by McDonald et al. (2009) (i.e., concentration, luminosity, surface brightness, and size). Moreover, while their distribution of r_{Min} is concentrated within 1.5 r_e , it is spread over a much wider range in terms of physical units (~ 0.5 –8.5 kpc). Thus, this special subpopulation of Virgo Type IIs cannot be linked to any specific disk galaxy structural properties.

⁹ Unfortunately, the luminosity profiles for VCC 664, 1555, and 1952 lacked sufficient flux to enable a measurement of their ages either up to (664 and 1952) or much beyond (1555) their breaks, so that the fraction of U-shaped age profiles in our Type II subsample may be as high as 45%.

Table 5
Morphologies, Effective Radii, Break Radii, and Age Minimum Radii
(When Present) for Virgo Type II Galaxies

VCC ID (1)	Hubble Type (2)	Profile Type ^a (3)	r_e (kpc) (4)	r_{Brk}		r_{Min}	
				(kpc) (5)	(r_e) (6)	(kpc) (7)	(r_e) (8)
0522	SAB(r)a	o-OLR+III	2.396	3.297	1.376
0596	SAB(s)bc	o-AB+III	8.398	8.242	0.981	8.554	1.019
0620	Sm	AB	1.157	0.577	0.497
0664	IB(s)m	o-CT	2.014	5.357	2.660
0792	S(rs)b	CT+III	4.019	5.769	1.434
0849	SAB(s)c	AB+III	1.720	2.102	1.222	1.790	1.041
0865	Sd	CT+III	6.716	5.522	0.822	5.188	0.773
0945	Im	AB	1.947	1.154	0.592
1021	IABm	i+III	1.273	0.824	0.604	0.587	0.428
1126	Sb	CT+III	2.280	3.297	1.445
1200	Im	AB	1.412	0.742	0.437
1508	SB(rs)d	o-CT+III	2.486	5.769	2.321
1532	SB(rs)c	o-AB+III	2.510	1.648	0.657
1555	SAB(s)c	o-AB	20.877	13.187	0.632
1654	IABm	o-AB	1.110	0.742	0.666	0.571	0.513
1696	S(r)d	CT+III	3.043	6.181	2.031
1726	Im	AB	1.738	1.484	0.838
1929	SAB(s)dm	o-OLR+III	2.871	2.225	0.775	1.664	0.580
1943	SAB(rs)bc	i+III	2.151	2.225	1.034	2.741	1.276
1952	Im	AB	0.959	1.154	1.204
1987	SAB(rs)cd	o-AB+III	4.940	6.593	1.335	8.554	1.732
2058	S(rs)bc	CT+III	4.026	4.533	1.126

Note. ^a i: break located within bar; o: break located outside bar; CT: classical truncation; AB: apparent/asymmetric break; OLR: break coincident with outer Lindblad resonance.

Table 5 also provides the morphologies and detailed luminosity profile classifications of our Type II galaxies, from which we infer that the Type II phenomenon amongst cluster galaxies is rarely associated with a bar. This should not necessarily be interpreted as suggesting that a bar has little effect on these galaxies' outskirts though, as a significant fraction of our Type II subsample bears morphological features which are consistent with previous bar activity (i.e., rings and lenses). Moreover, many of the latter systems exhibit U-shaped age profiles. The detailed profile classifications in Table 5 were determined following PT06's and Er08's scheme, whereby the designations "i" and "o" refer to the break occurring interior or exterior to the bar (if present), while "AB" and "OLR" indicate whether the break is related to either strong $m = 1$ outer-disk asymmetries or an outer Lindblad resonance (i.e., ring), respectively. If both the "AB" and "OLR" designations may be ruled out for any given galaxy, it is deemed to possess a classical truncation ("CT").¹⁰ The detailed classifications for our Type IIs show that this phenomenon within the cluster environment is most often attributed to an asymmetry in the disk ($f_{\text{AB}} = 0.5$), while classical truncations account for just under a third ($f_{\text{CT}} = 0.33$) of the Type II breaks we detect. The distribution of detailed Type II classes amongst Virgo disks also appears to be at odds with observations for field disks (albeit for late-type morphologies alone), for which most Type II breaks represent classical

¹⁰ It should be noted that the Type II classification scheme created by PT06 and Er08 was intended to provide a framework under which the origins of such galaxies could be understood; that is, it is largely hypothetical. For instance, whether the breaks in Type II-o.OLR disks actually occur at their outer Lindblad resonances has yet to be explicitly demonstrated vis-à-vis measurements of bar pattern speeds. Thus, our detailed classifications of the breaks in Virgo Type IIs should be interpreted with caution.

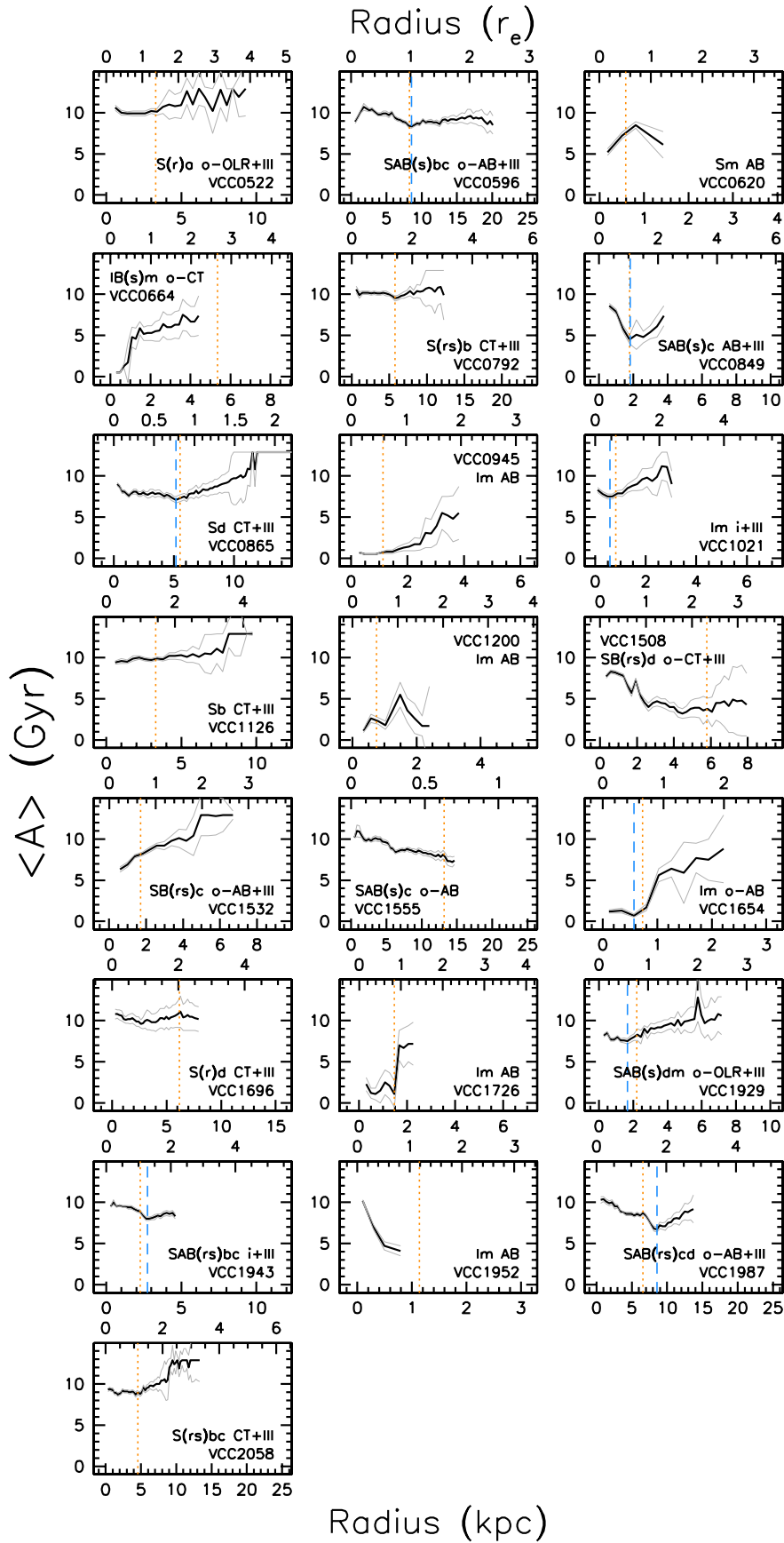


Figure 6. As in Figure 5 but for Virgo Type II galaxies and now the ranges along the horizontal axes match those used in the corresponding panels of Figure 3. The specific class of Type II break for each galaxy is also provided in each panel, while its location is marked by the orange vertical line. (A color version of this figure is available in the online journal.)

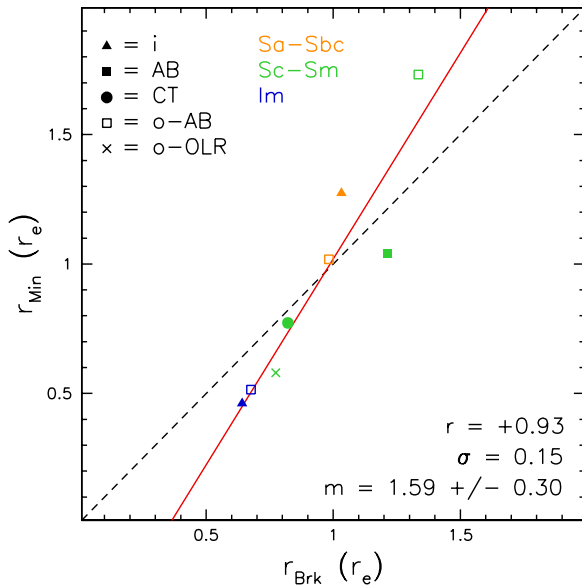


Figure 7. Location of age profile minima (r_{Min}) vs. location of luminosity profile breaks (r_{Brk}) for those Virgo Type II galaxies exhibiting age profile inversions. Both radii are scaled in terms of the galaxies’ H -band effective radii (r_e). The dashed line marks the 1:1 correlation. The data points are colored according to the galaxies’ morphologies (Sa–Sbc = orange, Sc–Sm = green, Im = blue), while the point types reflect the Type II class (triangle = i, circle = CT, square = o–AB, cross = o–OLR). The Pearson correlation coefficient, rms dispersion, and bootstrap linear fit slope (red line) are also provided.

truncations ($f_{\text{CT}} = 0.5$), followed by disk asymmetries and resonances in roughly equal proportions ($f_{\text{AB/OLR}} = 0.2$; PT06). This discrepancy, however, may also be accounted for by the nature of our sample since cluster galaxies have likely suffered tidal interactions more often throughout their evolution than field galaxies (and would therefore host asymmetric disks), which is to suggest that dense galaxy environments preferentially favor the development of different Type II classes (unlike findings for field spirals).

For those Type II galaxies in our subsample which exhibit U-shaped age profiles, we wish to compare the locations of their age minima against those of their breaks, given that simulations of Type II-CT disks in the field suggest that these locations should coincide (i.e., the luminosity profile break and age profile inversion phenomena are causally connected). We plot in Figure 7 the bivariate distribution of r_{Min} against r_{Brk} for the eight Virgo Type IIs which exhibit statistically significant age minima, where the dashed line is a one-to-one relation. For simplicity, we have plotted the two sets of locations in terms of these galaxies’ H -band effective radii. The points are colored according to galaxy morphologies (orange = Sa–Sbc, green = Sc–Sm, blue = Im), while the point types correspond to detailed Type II classifications (triangle = i, circle = CT, square = AB, cross = OLR), with open and solid points denoting barred and unbarred systems, respectively.

Figure 7 shows a clear correlation between the breaks and age minima locations for Type II galaxies in the Virgo cluster. A bootstrap linear fit to the data yields a Pearson correlation coefficient of $r = +0.92$ and a slope of $+1.59 \pm 0.30$. The existence of such a correlation, never reported before, expands on results from Type-II CT disk formation simulations by suggesting that U-shaped age profiles accompany the formation of *all* manner of Type II breaks in disk galaxies, particularly those whose breaks are associated with either a bar or disk

asymmetry (which drive the observed correlation). Whether all classes of Type II disks follow a unified $r_{\text{Min}}-r_{\text{Brk}}$ correlation is an issue to be explored further by models and observations aimed at a global understanding of the Type II phenomenon. For instance, it will be of interest to explore why the observed correlation is not one-to-one (the best-fit slope differs from unity at the 2σ level). Does the fact that r_{Min} falls either within or outside of r_{Brk} for most of the eight galaxies plotted in Figure 7 signal that some new mechanisms must be accounted for in future simulations? In this sense, it is noteworthy that Yoachim et al. (2012) find that two of their three U-shaped age profile detections have the minima occurring well inside of these galaxies’ corresponding Type II-CT breaks. Conversely, the one Type II-CT from our sample which appears in Figure 7 lies almost directly on top of the 1:1 line, as found in simulations of this particular Type II class.

The existence of an $r_{\text{Min}}-r_{\text{Brk}}$ correlation amongst all Virgo Type II disks suggests that a common physical mechanism is responsible for both phenomena in any given Type II galaxy. In the case of classical truncations, R08 argued that the break in their simulated Type II disk resulted from the combination of angular momentum conservation within the collapsing gas cloud, an assumed surface density threshold for star formation and resonant scattering of stars to radii beyond the truncation of the galaxy’s star-forming disk. Since older stars would have more time to diffuse to greater distances than younger ones, R08 naturally found that the break in their galaxy coincided with an inversion in its age profile. On the other hand, while very similar mechanisms were considered in SB09’s simulation, these authors offered another explanation for the origin of their galaxy’s break, whereby the rapid decline in star formation beyond the break radius (also seen in R08) was due to the onset of a warp in the gas disk rather than angular momentum conservation (as in R08). Although radial migrations still deposited a significant number of stars beyond the break in SB09’s simulation, these authors identified that the age minimum in their simulated galaxy was robust to whether or not radial migrations are invoked. Unfortunately, we could not assess with our data the level at which radial migrations contribute to the $r_{\text{Min}}-r_{\text{Brk}}$ correlation reported here since each of the recent simulations of Type II disk formation predict U-shaped age profiles within them and have only addressed the case of classical truncations thus far.

While ours is not the first report of a connection between Type II breaks and U-shaped age profiles, we have found evidence to suggest that this connection extends to *all* classes of Type IIs (not just Type II-CTs) through explicit age determinations. To our knowledge, the only previous detections of U-shaped age profiles in Type IIs are from Yoachim et al. (2010, 2012). Other previous similar age gradient studies of disk galaxies either only treated one galaxy at a time (de Jong et al. 2007; Williams et al. 2009; Barker et al. 2011; Radburn-Smith et al. 2012) or were hampered by signal-to-noise constraints and uncertain age determinations (due to the age–metallicity degeneracy at optical wavelengths, which is lifted by use of near-infrared fluxes, as we have done here; Azzollini et al. 2008; Bakos et al. 2008).

If the observed $r_{\text{Min}}-r_{\text{Brk}}$ correlation among Virgo Type IIs truly indicates that the formation of Type II breaks and U-shaped age profiles is causally connected, then the paucity of age minima reported in Table 5 clearly demands an explanation (positive, flat, and negative gradients describe the age profiles for 36%, 14%, and 14% of our Type II subsample,

respectively). This absence is most acutely noticed amongst the seven Type II-CTs in our subsample since U-shaped age profiles seem to be a robust prediction from the multiple simulations of these galaxies' formation performed thus far, yet we find such a profile in only one of these systems (VCC 0865). Of course, our comparison could be flawed by the fact that those simulations all addressed Type II-CT formation within the field, while the environment in which our cluster galaxies reside likely plays a significant role in their evolution. It is, however, worth recalling that in their stellar population analysis of *field* Type IIs, Yoachim et al. (2012) found that three of their six systems also lack U-shaped age profiles. These two arguments then suggest that some mechanisms (perhaps environmentally triggered; e.g., harassment) either inhibit the formation of, or erase the age minima within, all Type II classes. For instance, the age profiles for five of the eight Virgo Type IIs exhibiting positive age gradients (VCC 0522, 0945, 1126, 1726, and 2058) are fairly flat in their interiors but climb to relatively old ages in their outskirts; perhaps these galaxies' age profiles once more closely resembled that of VCC 1987 (Figure 6). Therefore, two fundamental issues for the future exploration of Type II formation models prevail: (1) whether U-shaped age profiles are expected in all Type II galaxy classes and (2) under what conditions are such age profiles prevented or simply erased?

3.3. Type IIIs

The mean stellar age profiles for the remaining disk galaxy type in our sample, the Type IIIs (of which we have 22), are shown in Figure 8. Unfortunately, since Type III breaks typically occur at low surface brightnesses ($\sim 27\text{--}28$ mag arcsec $^{-2}$), our age profiles for these galaxies often fail to extend to, or much beyond, their break radii. Still, over the radial extent probed by their age profiles, we find that (similar to the case of our Type II subsample) Virgo Type IIIs are described by a variety of age gradients: 23% are flat, 32% are positive, 18% are negative, and 27% are U-shaped (Table 2); the inner and outer gradients measured for those galaxies having U-shaped age profiles are listed in Table 3, while the break and age inversion radii (where applicable) for our entire Type III subsample can be found in Table 6. Given that hydrodynamical simulations of Type III disk formation are scant (and predictions of their stellar population properties are sorely lacking; Younger et al. 2007), the only possible extrapolation to our observations is that a variety of age gradients likely implies a corresponding variety of formation channels. It will be of interest to see whether future Type III disk formation models can reproduce our observed age gradient distribution and if environmentally triggered processes (e.g., harassment) are needed to achieve such an agreement.

Arguably the most interesting result to come out of our inspection of the age profiles for Virgo Type IIIs is that a significant fraction (27%) of them exhibit statistically significant U-shapes, akin to those seen in formation models of Type II-CT disks. In this case, however, we find that the minima systematically occur well inside these galaxies' breaks, as judged from the locations of the orange (breaks) and blue (minima) lines in Figure 8. This agrees with Bakos et al. (2008), who found that the stacked (optical) color profile for Type IIIs in the field exhibits an inversion at roughly half the distance to their break radii. As for our Type Is and IIs, we verified (through bootstrap linear fits) that each of proposed minima in our Type III subsample were defined by statistically meaningful negative and positive age gradients leading into and out of them, respectively (Table 3).

Table 6
Morphologies, Effective Radii, Break Radii, and Age Minimum Radii
(When Present) for Virgo Type III Galaxies

VCC ID (1)	Hubble Type (2)	r_e (kpc) (3)	r_{Brk}		r_{Min}	
			(kpc) (4)	(r_e) (5)	(kpc) (6)	(r_e) (7)
0483	S(rs)c	3.551	9.885	2.784	4.176	1.176
0692	SB(rs)ab	2.372	4.943	2.083	2.984	1.258
0809	Sdm	2.252	5.769	2.562
0912	SB(rs)ab	2.461	12.356	5.022	1.942	0.789
1110	S(s)ab	3.955	20.605	5.209
1326	SB(s)a	2.084	4.531	2.174
1358	Sa	1.188	3.709	3.121
1379	SAB(s)d	3.260	8.238	2.527	3.818	1.171
1393	SBcd	1.742	4.121	2.365
1479	SB(rs)ab	1.839	4.119	2.240
1486	SAB(s)b	0.900	4.121	4.579
1575	IBm	2.143	2.883	1.346	0.568	0.265
1615	SB(rs)b	5.427	16.484	3.037
1686	IBm	2.750	9.061	3.295	1.485	0.540
1727	SAB(rs)b	4.563	18.123	3.972
1757	SAB(s)a	1.614	5.766	3.573
1811	SAB(rs)b	1.562	4.119	2.637	2.188	1.401
1972	SAB(rs)c	7.806	6.181	0.792
2012	Scd	2.416	5.766	2.387	3.214	1.330
2023	Sc	2.663	4.533	1.702
2042	SABd	1.930	2.059	1.067
2070	S(s)ab	2.742	9.066	3.306

Since simulations of Type II-CT formation suggest that radial migrations foster U-shaped age profiles within these galaxies, we might speculate that a similar process is responsible for such profiles within Type III disks. In fact, Younger et al. (2007) have shown that a Type III luminosity profile could be produced through a minor merger onto a gas-rich disk, whereby the stars found beyond the remnant's break come predominantly from the progenitor disk. Thus, the merger event effectively incites a migration of stars from the inner regions of the progenitor to the outer regions of the remnant. Assuming the progenitor forms inside-out, this migratory process should raise the mean age of stars in the remnant's outskirts, thus giving rise to a U-shaped age profile. A minor merger origin for Type III disks is further supported by the observation that five of the six Virgo Type IIIs exhibiting U-shaped age profiles also host bars, a phenomenon well known to be created, at least in part, by the pericenter passages of dwarf satellites. Furthermore, dynamical simulations of barred galaxies have revealed that an age minimum should appear in the vicinity of the bar's ultraharmonic and outer Lindblad resonances (Wozniak 2007). The bars in these Virgo Type IIIs may then have played a key role in driving the radial migrations that we suspect were a principal component of their formation and might also explain why their age minima are found well into their interior regions. Despite our best efforts though, understanding these observations would clearly benefit from more extensive Type III formation models.

3.4. The Role of Environment in Disk Galaxy Evolution

The data-model comparisons carried out in each of the three previous sections all point to the common interpretation that the evolution of disk galaxies is likely very different in field and cluster environments. While this idea is already well ingrained, our comparisons of the mean stellar age profiles for all types

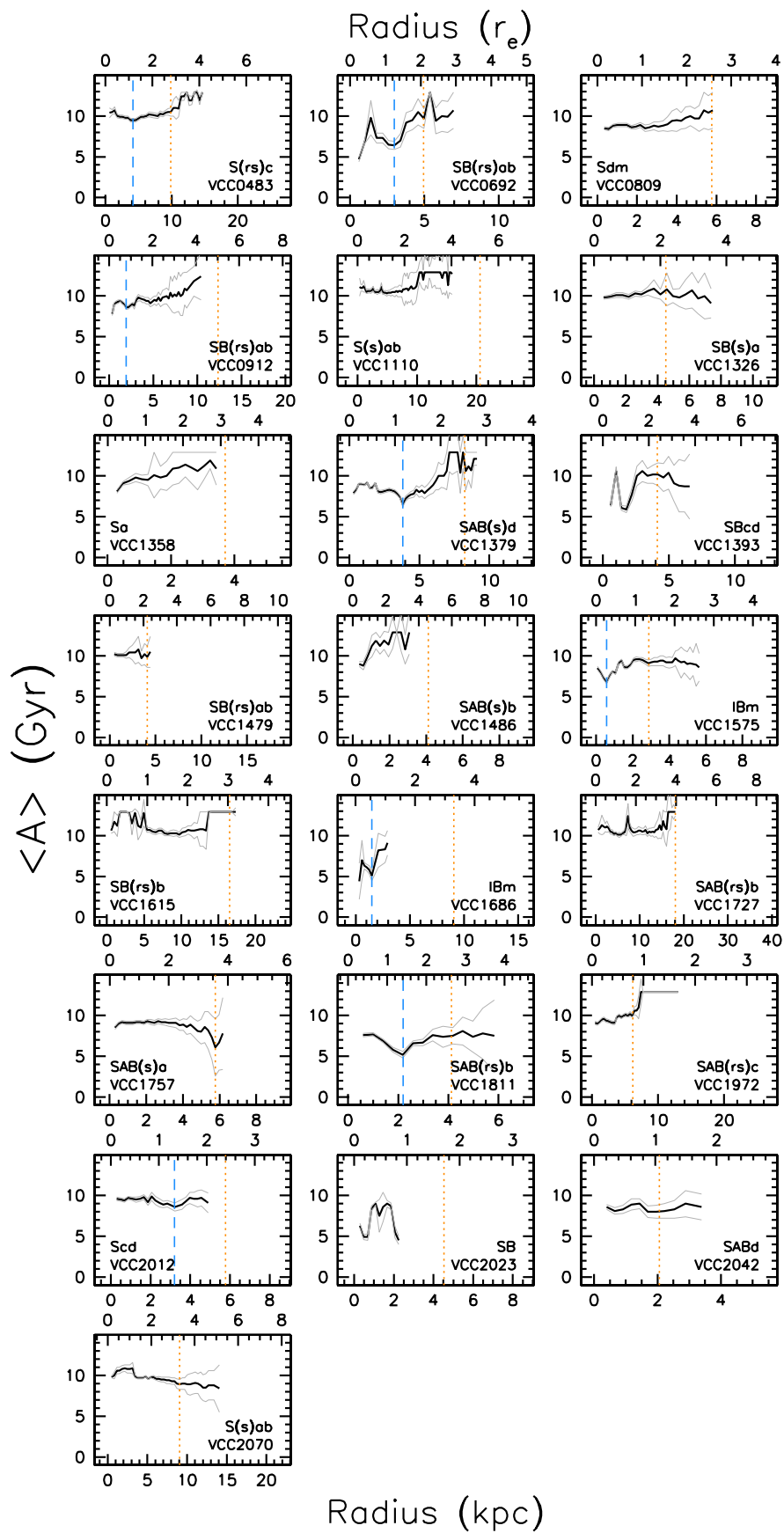


Figure 8. As in Figure 5 but for Virgo Type III galaxies and now the ranges along the horizontal axes match those used in the corresponding panels of Figure 4. The location of the break for each galaxy is marked by the orange vertical line in each panel. (A color version of this figure is available in the online journal.)

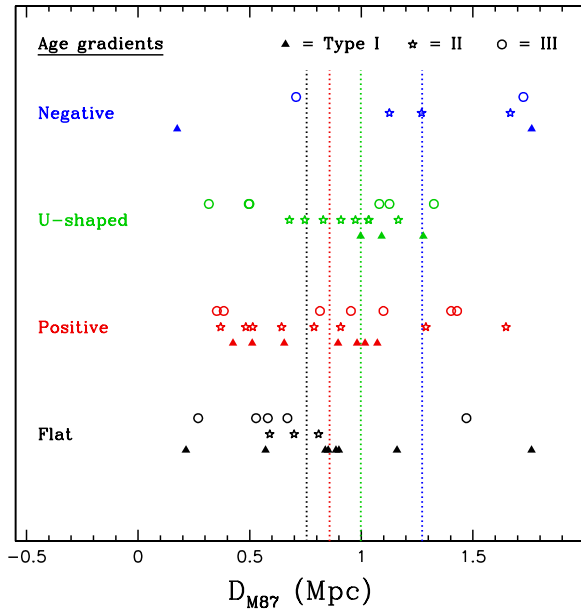


Figure 9. Differential distribution of (projected) cluster-centric radii for our Virgo disk galaxy sample. Galaxies have been binned and colored according to their age gradients (flat = black, positive = red, negative = blue, U-shaped = green). The point types refer to their luminosity profile shapes (Type I = triangle, II = star, III = circle). The colored vertical lines locate the median values of the four distributions.

of Virgo disk galaxies against predictions from hydrodynamic simulations for field galaxies (and along with the fractions of each disk Type as a function of environment; Section 2) further bolster this claim.

Our argument can be extended with a plot in Figure 9 of the differential distribution of (projected) cluster-centric radii for our entire Virgo disk galaxy sample, where galaxies have been binned and colored according to their age gradients (flat, positive, negative, and U-shaped). The point types represent their luminosity profiles shape: Types I, II, and III. The colored vertical lines correspond to the median value of each distribution. Despite global projection effects, Figure 9 shows that Virgo cluster galaxies with flat and positive age gradients are located preferentially closer to the cluster center than those with negative and U-shaped gradients. Given our expectations that, in the field, Type I disks would harbor negative age gradients and Type II and III disks would have U-shaped gradients, a simple overall explanation is that all of these galaxies initially formed like their field counterparts, but upon entering the cluster, their (local) environments transformed their age gradients into flat and/or positive ones. Conceptually speaking, such a transformation could be induced by ram-pressure stripping and harassment, processes which would conceivably quench the star formation in these galaxies’ outer disks (thereby raising the mean stellar age there) and radially mix the stellar populations throughout their disks (thereby flattening any pre-existing gradients). In order to better understand the observations presented here though, environmentally driven processes must be considered in future simulations of disk galaxy formation. Moreover, the observational case for a cluster-centric radial dependence of age gradients in disk galaxies could be improved (or disproved as the case may be) with deep, multiband imaging for a larger sample of cluster galaxies with more accurate distances (Ferrarese et al. 2012).

4. CONCLUSIONS

We have analyzed the luminosity and mean stellar age profiles for a complete, magnitude-limited sample of disk galaxies drawn from the Virgo cluster and shown that each of the three major disk galaxy types in this cluster can harbor statistically meaningful inversions (“U-shapes”) in their age profiles, akin to those predicted by recent high-resolution simulations of Type II disk galaxy formation in the field (Roškar et al. 2008; Martínez-Serrano et al. 2009; Sánchez-Blázquez et al. 2009). Since the inversions found in the simulated galaxies were formed, in part, by radial migrations of disk stars (and lacking guidance from simulations of cluster galaxies), we speculate that stellar migrations are a generic feature of galaxy formation, independent of both the disk galaxy type and the particular agent by which migrations are achieved (i.e., bar, spiral arm, and satellite). However, the fact that all of our cluster disk galaxies, most notably six of our seven classically truncated Type II (as well as disks found in *field* environments; Yoachim et al. 2012), do not exhibit inversions in their age profiles and given the reduced fraction of Type II systems in the Virgo cluster relative to the field, suggests that the significance of stellar migrations is likely sensitive to other prominent factors involved in galaxy evolution, such as environmentally driven processes in clusters (e.g., harassment). Equally interesting is that, in the absence of U-shaped age profiles, most of our galaxies are described by age profiles having either flat or positive gradients, as opposed to the negative gradients generically predicted by formation models of exponential disks. We still interpret this observation as supporting a picture of disk galaxy evolution where environment plays a principal role.

We have also shown that, for those Type II cluster galaxies in our sample that exhibit significant inversions in their age profiles, the locations of their luminosity profile breaks and age minima are correlated. This finding tentatively confirms the predictions of simulations of classically truncated Type II (Roškar et al. 2008; Martínez-Serrano et al. 2009; Sánchez-Blázquez et al. 2009) and sets the stage for further simulation work since the above correlation suggests that process(es) causing *all* manners of Type II breaks in disk galaxies would also generate inverted age profiles. However, while the simulations imply a direct (1:1) correspondence between the light profile break and age inversion radii, we find a significantly steeper slope (1.6 ± 0.3) for those two parameters. This result may indicate additional physics at play in the age profile inversion phenomenon or simply reflect some uncertainty in our (visual) assessment of those breaks and/or minima. Still, although our hypothesis for a *unified* “light profile break–age profile inversion” correlation amongst all Type II disks is new, it complements previous findings of age inversions in *classically truncated* Type II disks well inside of their respective breaks.

Our results on the stellar populations of all three disk galaxy types within the cluster environment pose a challenge to current galaxy formation models, which we are likely explained by environmentally induced evolutionary processes still missing in such models. In particular, future models may possibly reproduce the distribution of disk galaxy types and the respective mixture of age gradients in cluster galaxies once effects like ram-pressure stripping and harassment have been accounted for.

In the Appendix, we concur with Erwin et al. (2012) that Type II breaks are seemingly absent in cluster S0 galaxies. We also view many of their Type III classifications as either single $n > 1$ Sérsic profiles, bona fide disk upturns, or Type I

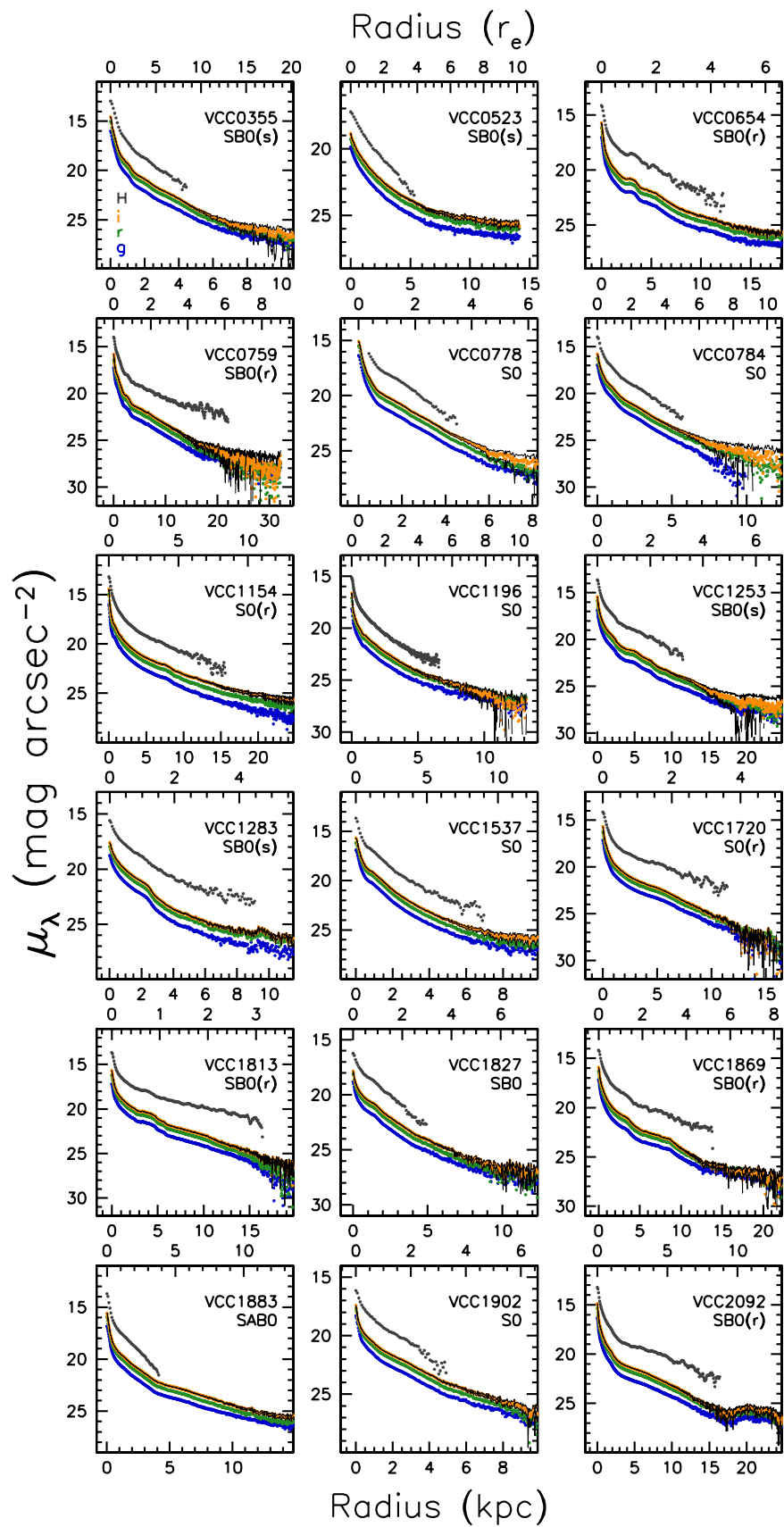


Figure 10. As in Figure 2 but for Virgo S0s common to both our entire sample and that of Erwin et al. (2012). (A color version of this figure is available in the online journal.)

disk systems with a faint stellar halo. The latter ought to be routinely detected in galaxy images reaching below $\mu_i \simeq 27$ mag arcsec $^{-2}$, as in M31 (Courteau et al. 2011).

We thank Peter Erwin, Kelly Foyle, Brad Gibson, and Robert Thacker for comments on an earlier version of this paper which led to valuable improvements. The referee’s thoughtful suggestions also improved the content and clarity of our paper. J.C.R. and S.C. acknowledge financial support from the National Science and Engineering Council of Canada through a postgraduate scholarship and a Discovery Grant, respectively. P.S.-B. is supported by the Ministerio de Ciencia e Innovacion (MICINN) of Spain through the Ramon y Cajal programme. P.S.-B. also acknowledges a Marie Curie Intra-European Reintegration grant within the Sixth European framework program. Support for this work was provided to M.M. by NASA through SAO Award Number 2834-MIT-SAO-4018, which is issued by the Chandra X-ray Observatory on behalf of NASA under contract NAS8-03060.

APPENDIX

ERWIN ET AL. (2012)

We noted in Section 2 that the 55 S0 galaxies from the McDonald et al. (2011) sample were left out of our analysis. This is due to the complicated interpretation of their surface brightness profiles where the bulge component is typically dominant. According to the near-infrared bulge–disk decompositions of McDonald et al. (2009), nearly two-thirds of the 55 S0s in our parent sample exhibit exponential-like profiles (within their sky error envelopes). Thus, without additional chemical or dynamical information, these structures could be viewed as either bulge- or disk-like. Given the inherent challenges with analyzing S0’s faint outer disks and their acute sensitivity to sky levels, accurate modeling of their bulges via multiband bulge–disk decompositions would be required in the pursuit of such a goal, a level of detail which lies beyond the scope of the present work (see also Prochaska Chamberlain et al. 2011).

Given the nontrivial interpretation of the outer disks in S0 galaxies, it seems prudent to examine the recent claims by Er12 about Virgo cluster S0 disks. Using optical imaging largely from the Sloan Digital Sky Survey (SDSS), as well as some of their own observations, Er12 compared the incidence of Type II breaks in field and cluster S0s to find that such features are entirely absent in the cluster S0s (at least down to a limiting surface brightness of $r \sim 27$ mag arcsec $^{-2}$). Rather, these authors find that the luminosity profiles of cluster S0s are evenly distributed between the Type I and III classes. Figure 10 shows the $griH$ surface brightness profiles for the 18 S0 galaxies from our parent sample which overlap with Er12’s Virgo sample. Our classification of pure exponential (Type I) luminosity profiles for VCC 654, 778, 784, 1253, 1720, 1813, and 2092 agrees with Er12. Other luminosity profile shapes, such as Er12’s Type IIIs, are, however, less clearly agreed upon. For instance, VCC 523, 1154, 1196, and 1537 have no discernible profile break or outer disk component and are modeled as a single Sérsic structure in McDonald et al. (2011); Er12 instead view them as Type III systems (with breaks located at 27”, 119”, 63”, and 29”). Er12 also identify Type III profiles (breaks) in VCC 355 (83”), 759 (190”), 1827 (54”), and 1902 (58”), yet our sky error envelopes, as shown in Figure 10, make them consistent with both a single exponential or a Type III disk. An issue with our profile shape assessments is the relatively low signal-to-noise ratio of the

SDSS images at levels where Type III breaks are normally detected.

Whether galaxies with outer profile upturns are viewed as a smooth Sérsic bulge plus a Type III disk or a Sérsic bulge plus a Type I disk and a stellar halo depends highly on the nature of the isophotal fitting in the inner parts (e.g., whether isophotes have concentric [Erwin] or variable [us] position angles), the accuracy of sky subtraction, and the ability to distinguish a stellar disk from a stellar halo.

This is not to say that disk profile upturns, or “anti-truncated” disks, are unexpected. These may result from a component which is actually independent from the disk itself, such as a stellar halo (e.g., as seen in M31; Courteau et al. 2011) or other accreted external material. Such profile upturns, or disk/halo transitions, are typically seen at surface brightnesses below $\mu_i \simeq 26$ – 27 mag arcsec $^{-2}$ (Courteau et al. 2011). With a typical limit of $\mu_i \simeq 26.5$ mag arcsec $^{-2}$ (Hall et al. 2012), our own SDSS profiles are barely deep enough to assess the presence of disk/halo structures. The latter is clearly of tremendous interest, though once again, beyond the scope of the present study.

Type III upturns may also be purely confined to the disk, as confirmed by spiral-arm structure which appears to extend beyond the Type III break radius (e.g., NGC 3982 in Erwin et al. 2008; see their Figure 11). Models that explain Type III disks via mechanisms other than pure accretion include harassment or minor mergers. The harassment simulations of Moore et al. (1999) show clearly the evolution of a Type I disk into a Type III system. The minor merger models of Younger et al. (2007) also show that the “outer light excess” comes from disk stars in the original primary galaxy that gained angular momentum from the minor merger process. All things considered, though, the generation of a Type III profile always requires an external agent.

In summary, while we do not find Type III systems in our Virgo cluster sample of S0 galaxies (McDonald et al. 2011), we concur with Er12’s important claim that Type II breaks are seemingly absent in S0 cluster galaxies. The latter is confirmed by examination of our Virgo cluster sample (McDonald et al. 2011).

REFERENCES

- Abadi, M. G., Moore, B., & Bower, R. G. 1999, *MNRAS*, 308, 947
 Azzollini, R., Trujillo, I., & Beckman, J. E. 2008, *ApJ*, 679, L69
 Bakos, J., Trujillo, I., & Pohlen, M. 2008, *ApJ*, 683, L103
 Barker, M. K., Ferguson, A. M. N., Cole, A. A., et al. 2011, *MNRAS*, 410, 504
 Binggeli, B., Sandage, A., & Tammann, G. A. 1985, *AJ*, 90, 1681
 Bird, J. C., Kazantzidis, S., & Weinberg, D. H. 2012, *MNRAS*, 420, 913
 Bland-Hawthorn, J., Vlahić, M., Freeman, K. C., & Draine, B. T. 2005, *ApJ*, 629, 239
 Bournaud, F., Elmegreen, B. G., & Elmegreen, D. M. 2007, *ApJ*, 670, 237
 Courteau, S., Widrow, L. M., McDonald, M., et al. 2011, *ApJ*, 739, 20
 Debattista, V. P., Mayer, L., Carollo, C. M., et al. 2006, *ApJ*, 645, 209
 de Grijs, R., Kregel, M., & Wesson, K. H. 2001, *MNRAS*, 324, 1074
 de Jong, R. S., Seth, A. C., Radburn-Smith, D. J., et al. 2007, *ApJ*, 667, L49
 Dressler, A. 1980, *ApJ*, 236, 351
 Dutton, A. A. 2009, *MNRAS*, 396, 121
 Edvardsson, B., Andersen, J., Gustafsson, B., et al. 1993, *A&A*, 275, 101
 Elmegreen, B. G., & Parravano, A. 1994, *ApJ*, 435, L121
 Erwin, P., Beckman, J. E., & Pohlen, M. 2005, *ApJ*, 626, L81
 Erwin, P., Gutiérrez, L., & Beckman, J. E. 2012, *ApJ*, 744, L11 (Er12)
 Erwin, P., Pohlen, M., & Beckman, J. E. 2008, *AJ*, 135, 20 (Er08)
 Fall, S. M., & Efstathiou, G. 1980, *MNRAS*, 193, 189
 Ferguson, A. M. N., & Clarke, C. J. 2001, *MNRAS*, 325, 781
 Ferrarese, L., Côté, P., Cuillandre, J.-C., et al. 2012, *ApJS*, 200, 4
 Foyle, K., Courteau, S., & Thacker, R. J. 2008, *MNRAS*, 386, 1821

- Freeman, K. C. 1970, *ApJ*, **160**, 811
- Gavazzi, G., Boselli, A., van Driel, W., & O’Neil, K. 2005, *A&A*, **429**, 439
- Gil de Paz, A., Madore, B. F., Boissier, S., et al. 2005, *ApJ*, **627**, L29
- Gutiérrez, L., Erwin, P., Aladro, R., & Beckman, J. E. 2011, *AJ*, **142**, 145
- Hall, M., Courteau, S., Dutton, A. A., McDonald, M., & Zhu, Y. 2012, *MNRAS*, submitted
- Haynes, M. P., & Giovanelli, R. 1984, *AJ*, **89**, 758
- Haywood, M. 2008, *MNRAS*, **388**, 1175
- Kennicutt, R. C., Jr. 1989, *ApJ*, **344**, 685
- Lin, D. N. C., & Pringle, J. E. 1987, *ApJ*, **320**, L87
- Maltby, D. T., Gray, M. E., Aragón-Salamanca, A., et al. 2012, *MNRAS*, **419**, 669
- Martínez-Serrano, F. J., Serna, A., Doménech-Moral, M., & Domínguez-Tenreiro, R. 2009, *ApJ*, **705**, L133 (MS09)
- McCarthy, I. G., Frenk, C. S., Font, A. S., et al. 2008, *MNRAS*, **383**, 593
- McDonald, M., Courteau, S., & Tully, R. B. 2009, *MNRAS*, **394**, 2022
- McDonald, M., Courteau, S., Tully, R. B., & Roediger, J. 2011, *MNRAS*, **414**, 2055
- Mei, S., Blakeslee, J. P., Côté, P., et al. 2007, *ApJ*, **655**, 144
- Minchev, I., & Famaey, B. 2010, *ApJ*, **722**, 112
- Mollá, M., & Díaz, A. I. 2005, *MNRAS*, **358**, 521
- Moore, B., Katz, N., Lake, G., Dressler, A., & Oemler, A. 1996, *Nature*, **379**, 613
- Moore, B., Lake, G., Quinn, T., & Stadel, J. 1999, *MNRAS*, **304**, 465
- Naab, T., & Ostriker, J. P. 2006, *MNRAS*, **366**, 899
- Nordström, B., Mayor, M., Andersen, J., et al. 2004, *A&A*, **418**, 989
- Pohlen, M., Dettmar, R.-J., Lütticke, R., & Aronica, G. 2002, *A&A*, **392**, 807
- Pohlen, M., & Trujillo, I. 2006, *A&A*, **454**, 759 (PT06)
- Prochaska Chamberlain, L. C., Courteau, S., McDonald, M., & Rose, J. A. 2011, *MNRAS*, **412**, 423
- Quillen, A. C., Minchev, I., Bland-Hawthorn, J., & Haywood, M. 2009, *MNRAS*, **397**, 1599
- Radburn-Smith, D. J., Roškar, R., Debattista, V. P., et al. 2012, *ApJ*, **753**, 138
- Robertson, B., Yoshida, N., Springel, V., & Hernquist, L. 2004, *ApJ*, **606**, 32
- Roediger, J. C., Courteau, S., MacArthur, L. A., & McDonald, M. 2011a, *MNRAS*, **416**, 1996
- Roediger, J. C., Courteau, S., McDonald, M., & MacArthur, L. A. 2011b, *MNRAS*, **416**, 1983
- Roediger, E., & Hensler, G. 2005, *A&A*, **433**, 875
- Roškar, R., Debattista, V. P., Stinson, G. S., et al. 2008, *ApJ*, **675**, L65 (R08)
- Sánchez-Blázquez, P., Courty, S., Gibson, B. K., & Brook, C. B. 2009, *MNRAS*, **398**, 591 (SB09)
- Schaye, J. 2004, *ApJ*, **609**, 667
- Sellwood, J. A., & Binney, J. J. 2002, *MNRAS*, **336**, 785
- Slyz, A. D., Devriendt, J. E. G., Silk, J., & Burkert, A. 2002, *MNRAS*, **333**, 894
- Spitzer, L., Jr. & Schwarzschild, M. 1953, *ApJ*, **118**, 106
- Thilker, D. A., Bianchi, L., Meurer, G., et al. 2007, *ApJS*, **173**, 538
- van den Bosch, F. C. 2001, *MNRAS*, **327**, 1334
- van der Kruit, P. C. 1979, *A&AS*, **38**, 15
- van der Kruit, P. C. 1987, *A&A*, **173**, 59
- Vlajić, M., Bland-Hawthorn, J., & Freeman, K. C. 2009, *ApJ*, **697**, 361
- Vollmer, B., Cayatte, V., Balkowski, C., & Duschl, W. J. 2001, *ApJ*, **561**, 708
- Wielen, R. 1977, *A&A*, **60**, 263
- Wielen, R., Fuchs, B., & Dettbarn, C. 1996, *A&A*, **314**, 438
- Williams, B. F., Dalcanton, J. J., Dolphin, A. E., Holtzman, J., & Sarajedini, A. 2009, *ApJ*, **695**, L15
- Wozniak, H. 2007, *A&A*, **465**, L1
- Yoachim, P., Roškar, R., & Debattista, V. P. 2010, *ApJ*, **716**, L4
- Yoachim, P., Roškar, R., & Debattista, V. P. 2012, *ApJ*, **752**, 97
- Younger, J. D., Cox, T. J., Seth, A. C., & Hernquist, L. 2007, *ApJ*, **670**, 269